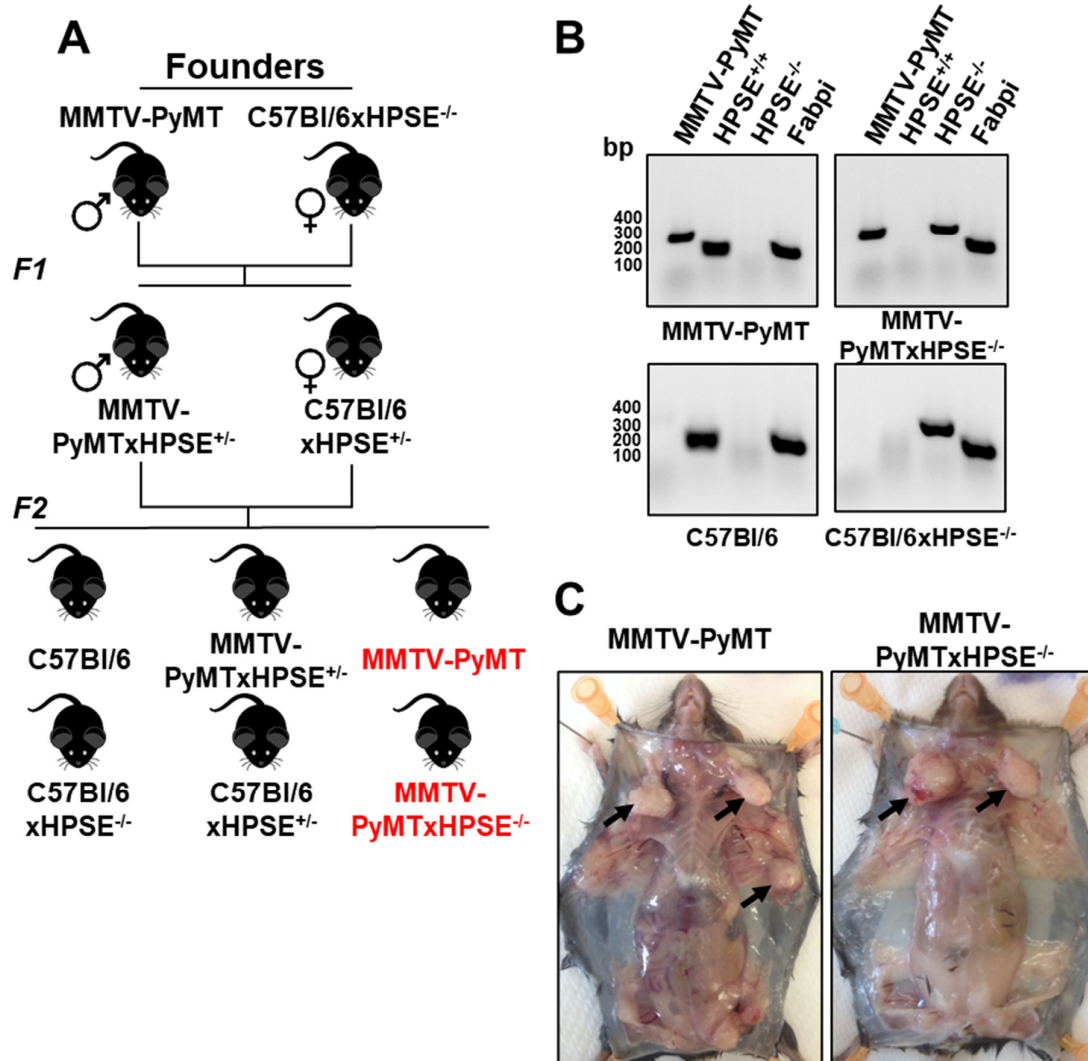
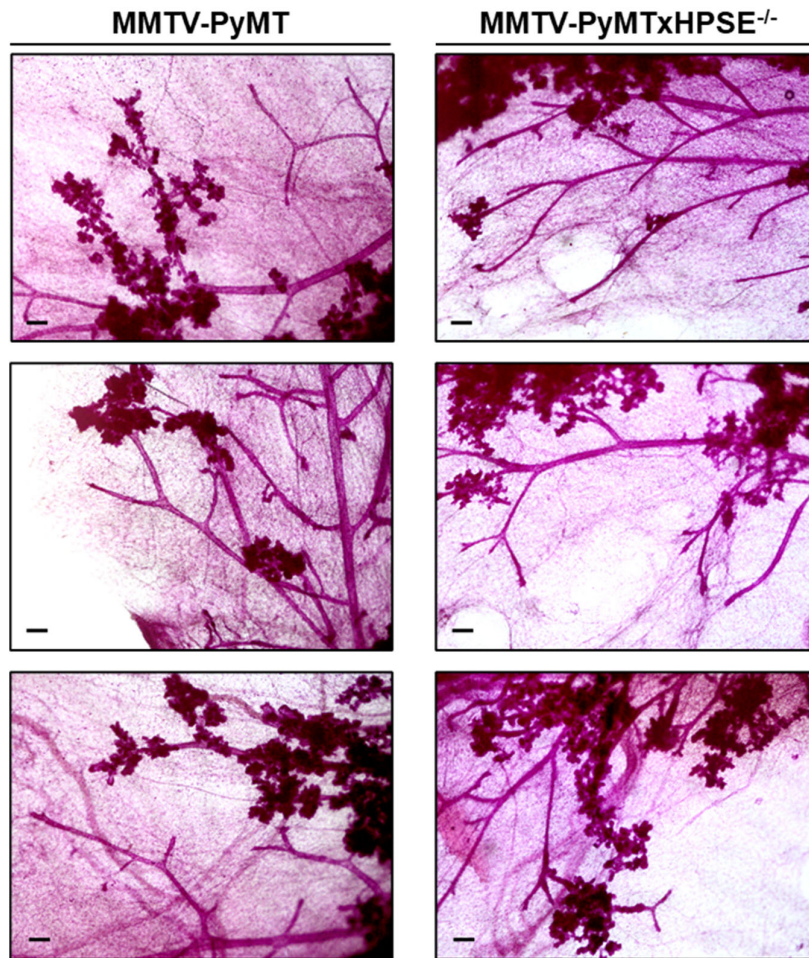


Supplementary Materials



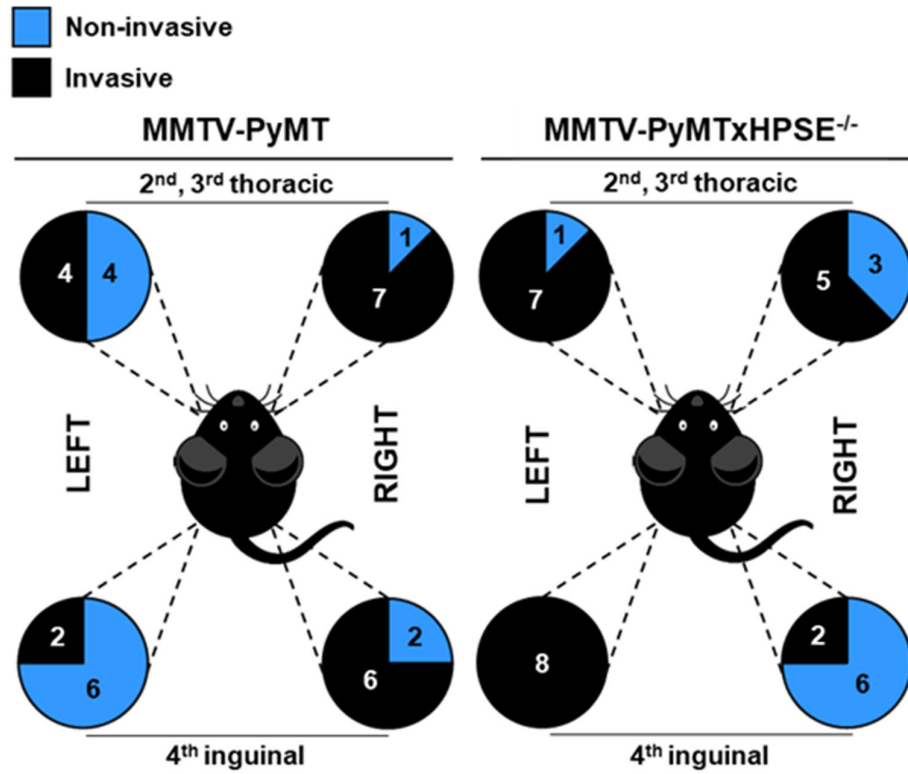
Supplementary Figure S1. The generation of MMTV-PyMTxHPSE^{-/-} mice

(A) The schematic of the breeding strategy used to generate MMTV-PyMTxHPSE^{-/-} mice. The genetic backgrounds of animals resulting from the F2 generation that were used in subsequent *in vivo* studies are indicated in red. **(B)** Genotypes of MMTV-PyMT, MMTV-PyMTxHPSE^{-/-}, C57BI/6 and C57BI/6xHPSE^{-/-} animals were confirmed by PCR. **(C)** Representative photographs of spontaneous mammary tumour-bearing female MMTV-PyMT and MMTV-PyMTxHPSE^{-/-} mice at 20-weeks of age, showing visible mammary tumours (arrows).



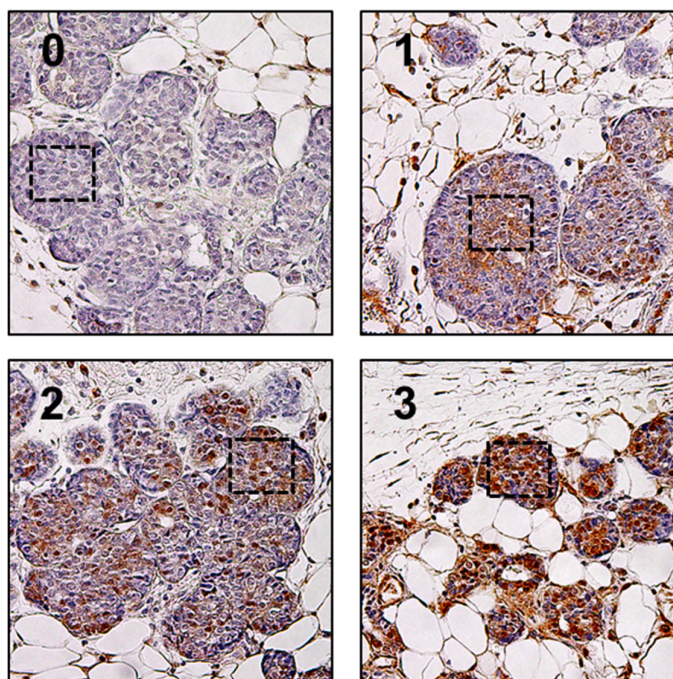
Supplementary Figure S2. Mammary gland architecture of MMTV-PyMT and MMTV-PyMTxHPSE^{-/-} mice at the ethical tumour volume end point

Whole-mounted 4th inguinal mammary glands of MMTV-PyMT and MMTV-PyMTxHPSE^{-/-} mice excised at the ethical tumour volume end point appeared similar in architecture upon visual observation. Representative images of one mammary gland per mouse, $n = 3$ per group. Scale bars = 50 μm .



Supplementary Figure S3. The role of HPSE in early mammary tumour development in MMTV-PyMT and MMTV-PyMTxHPSE^{-/-} mice

A pie-chart representation of invasive vs non-invasive phenotypes observed in each of the excised mammary glands of MMTV-PyMT and MMTV-PyMTxHPSE^{-/-} mice as reported in figure 6 ($n = 8$).



Supplementary Figure S4. H-scoring of mammary tumour sections following IHC staining

A score of 0 – 3 was assigned to four distinct levels of staining, from no staining to highest intensity.

Supplementary Figure S5. Original Western Blots for Figure 1A.

